

中国机构 CNS月报

01月刊

生物探索出品

目 录

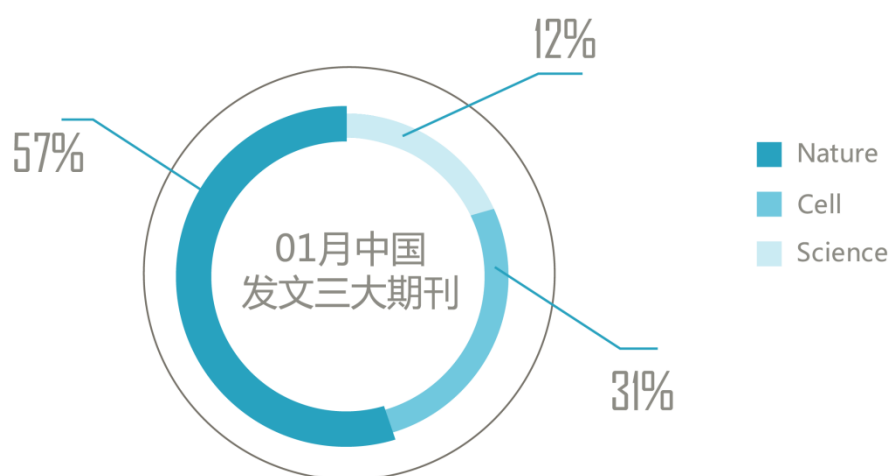
一、导语.....	1
二、1 月份中国机构发文 CNS 三大期刊.....	1
三、1 月份学术领域热度.....	2
四、1 月份城市&地区在 CNS 的论文和影响因子.....	3
五、1 月份中国机构发文 CNS 的走势.....	4
六、1 月份 CNS 发文机构论文量统计.....	5
七、1 月份 CNS 论文通讯作者的项目数和经费.....	6
八、专家简谈.....	7
九、1 月份论文列表.....	10
1、Nature 及其子刊.....	10
2、Cell 及其子刊.....	19
3、Science 及其子刊.....	23

一、导语

令国内科研界振奋的是，自然系列期刊在 2012 年的论文统计显示，发文 140 篇论文的中国科学院超过日本东京大学排名亚洲机构第一位，这也是 Nature Index 统计以来中国科研机构首次排名第一，反映出中国顶尖科研机构在数量上领跑亚洲。据生物探索统计，近 3 年内中国科研机构在 Nature、Cell 和 Science 三大系列期刊的总发文量逐渐上升，由 2010 年的 140 篇上升到 2011 年的 199 篇，再升至 2012 年的 262 篇。在 2012 年，中国机构发文 Nature 系列期刊 157 篇，Cell 系列期刊 126 篇和 Science 系列期刊 73 篇。

在生物学领域，三大期刊（Cell、Nature 和 Science）及其子刊，简称 CNS，倍受中国研究人员推崇，他们希望凭借 CNS 在学术界的威望将中国最尖端、最前沿的研究成果向全世界传达。这些研究动态可谓是中国科研机构的最高水平。作者希望对此进行统计，以便于从发文成果追踪国内科研经费动向，同时，生物医药圈内的研究人员和学生可实时了解中国顶尖研究人员从事研究的领域和方向。

二、1 月份中国机构发文 CNS 三大期刊

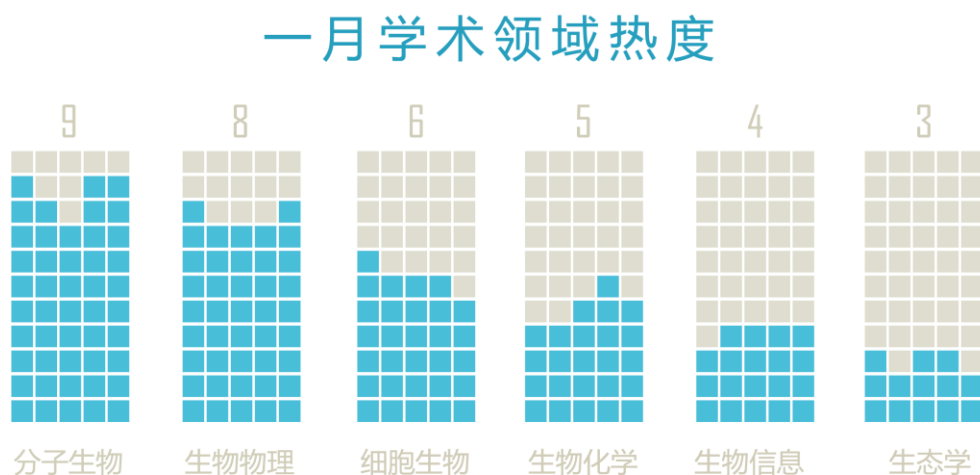


（饼状图表示期刊论文百分数）

2013 年 1 月份中国研究机构在三大期刊及其子刊共发表 35 篇论文,包括 Nature 系列 20 篇、Cell 系列 11 篇和 Science 系列 4 篇。其中 Nature、Cell 和 Science 主刊的发文量分别是 3、4 和 3 篇,在各自系列的比例分别是 15%、36.3%和 75%。值得注意的是,Cell 主刊 1 月份连发的 3 篇论文打破了继 2012 年 8 月份之后中国机构论文无缘 Cell 主刊的困境,这一成绩在 2012 年 Cell 主刊总共发表中国机构 10 篇论文的背景下尤其突出。

继 12 月份港台地区共发表 4 篇 CNS 论文之后,2013 年 1 月份该地区共发表 5 篇 CNS 论文(香港 3 篇,台湾 2 篇)。在论文影响因子方面,港台地区贡献了 75.2 分,约占总影响分子 641.7 分的 11.7%。其余的 30 篇都源自中国大陆,这反映出其研究机构在 CNS 论文方面处于主体地位。

三、1 月份学术领域热度



(柱状图反映论文数量/篇)

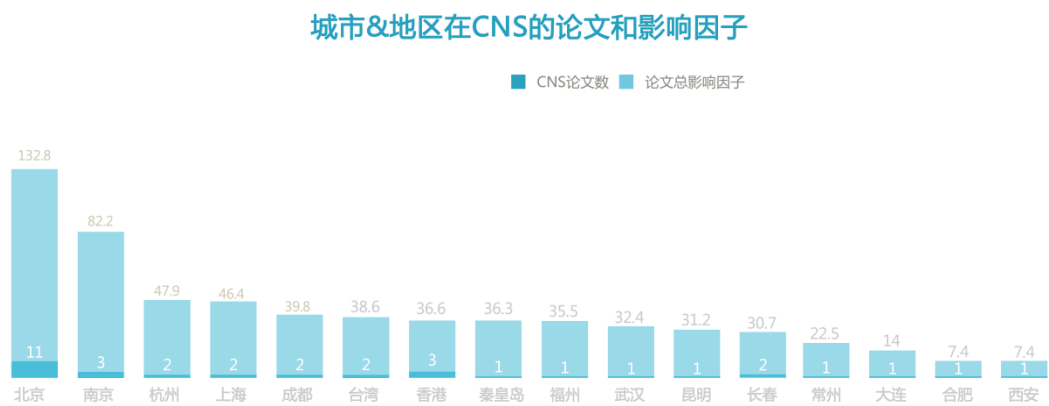
在 1 月份 CNS 刊登的中国研究论文中,分子生物学拥有 9 篇论文仍处于榜首,生物信息学分别位于。从来源上看,分子生物学论文在 Nature、Cell 和 Science 系列期刊上分别为 5 篇、4 篇和 1 篇,其中在 Cell 系列期刊占最大比例,达到 80%。

在 1 月份 CNS 刊登的中国研究论文中,分子生物学以 10 篇列于榜首,生物物理和细胞生物分别位于第二、第三位。从来源上看,分子生物学论文在 Nature 和 Cell 系列期刊上为 3 篇

和 6 篇，分别占到 15% 和 54.5%。

以基因组为对象的生物信息学研究持续成为热点，近 5 个月内都有关于基因组测序的 CNS 论文发表。在 4 篇生物信息学论文中，基因组方面论文占到 1 篇（蛾的遗传组成和食草性进化）。

四、1 月份城市&地区在 CNS 的论文和影响因子



（影响因子源自 MedSci 查询系统，取小数点后一位）

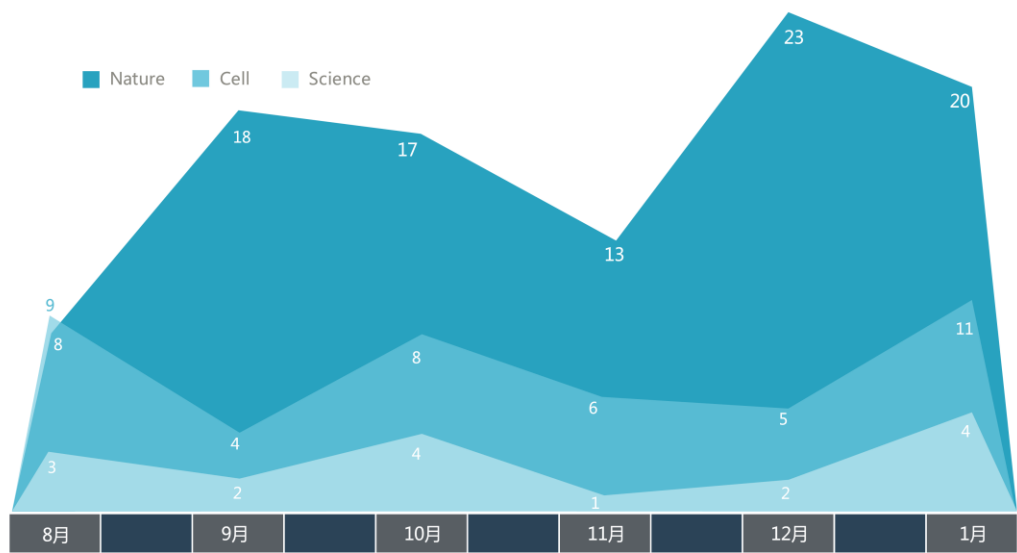
从城市&地区来看，1 月份 CNS 论文影响因子超过 100 分的仅有北京一地，北京以 132.8 分卫冕排行榜，较上月跌幅达 144 %。占据第二位的南京上个月没有发表 CNS 论文，而本月凭借 3 篇论文得到 82.2 分。从上图可以看出，北京的 CNS 论文影响因子遥遥领先其它城市&地区。

1 月份，发表 3 篇 CNS 论文的香港地区获得的影响因子是 36.6 分，还没有仅发表 2 篇的杭州、上海、成都和台湾的影响因子高；而发表 2 篇 CNS 的长春得到 30.7 分，却没有发表 1 篇的秦皇岛、福州、武汉和昆明的影响因子高；另外，常州、大连、合肥和西安都在 1 月份都发表一篇 CNS 论文。

对城市&地区的 CNS 影响因子统计，生物探索网站希望向用户提供关于地区研究水平的一项指数，让科研人员在从事各自研究领域的同时选择较高的研究平台和学术氛围。此外，由

于论文来自不同的经费项目，因此城市&地区的 CNS 影响因子能从一个方面反映国家经费的分配比例。

五、1 月份中国机构发文 CNS 的走势



中国机构发文CNS的走势

（数据统计源自 NCBI 网站 Pubmed）

在 2012 年 8 月至 2013 年 1 月之间中国机构发文 CNS 的统计结果中，数据表明：Nature 及其子刊发表的中国研究论文数量处于高位，总计 99 篇，其中 12 月最高达到 23 篇；相反，Science 及其子刊发表的中国研究论文数量处于低位，总计 16 篇，其中 11 月最低下落至 1 篇。

Nature 系列期刊的数量最多，它覆盖的学术类别和影响因子也较多，这是中国研究论文发表在 Nature 系列刊最多的原因之一；另一原因可能是，Nature 系列期刊对中国机构的研究成果认可度高，从 Nature 在上海设立编辑部一事可以看出，它对中国机构研究成果的重视。

六、1 月份 CNS 发文机构论文量统计

研究机构	CNS 论文		
	1 月份发文量	近 5 年总数	总数
中国科学院上海生物研究所	1	62	90
清华大学	4	56	71
北京大学	1	36	45
香港科技大学	1	22	38
复旦大学	1	29	37
香港大学	2	25	31
中国科学技术大学	1	21	28
中国农业大学	1	10	16
浙江大学	1	13	15
台湾国立清华大学	1	5	15
武汉大学	1	11	14
中国科学院物理研究所	1	8	13
中国科学院动物研究所	1	10	13
中国科学院化学研究所	1	7	8
吉林大学	1	4	7
南京师范大学	1	3	6
四川大学	1	3	5
中国科学院微生物研究所	1	5	5
西安交通大学	1	5	5
东南大学	2	4	4
中国科学院昆明植物研究所	1	4	4
四川农业大学	1	2	2
常州大学	1	1	1
国立台湾科技大学	1	1	1
首都医科大学	1	1	1
大连理工大学	1	1	1
燕山大学	1	1	1
福建农林大学	1	1	1
东北师范大学	1	1	1
杭州师范大学	1	1	1

（数据源于 NCBI 网站 Pubmed）

从 1 月份 CNS 中国机构论文总数榜单上看，排名前三的分别上海生命科学研究院、清华大

学和北京大学，上个月，它们同样排在前三。发表 1 篇 CNS 论文以上的研究机构是清华大学、香港大学和东南大学，其中清华大学发表了 4 篇，是本月最高发文量的单位。

在 1 月份 CNS 论文的统计数据中，除台湾国立清华大学之外，中国机构近 5 年发表的 CNS 论文总数全都不低于其 CNS 论文总数的一半，这表明近 5 年来中国机构发文 CNS 的速度和数量增加较快；1 月份 10 家研究机构首次发文 CNS，它们是中国科学院昆明植物研究所、四川农业大学、常州大学、国立台湾科技大学、首都医科大学、大连理工大学、燕山大学、福建农林大学、东北师范大学和杭州师范大学；除首次发文 CNS 的研究机构外，中国科学院微生物研究所、西安交通大学、东南大学、中国科学院昆明植物研究所和四川农业大学发表的 CNS 论文全都在近 5 年内。

七、1 月份 CNS 论文通讯作者的项目数和经费

研究机构	通讯作者	项目金额/万	项目数/个
中国科学院化学研究所	万立骏	8970.2	17
中国人民解放军第二军医大学	曹雪涛	2796.4	17
燕山大学	田永君	1577	7
清华大学	陈晔光	1027.4	11
中国科学院遗传与发育所	傅向东	952.8	8
中国科学院微生物研究所	谭华荣	754.3	13
中国科学院上海生物研究所	王恩多	753.7	16
东南大学	熊仁根	549.4	9
东南大学	谢维	508	6
清华大学	王亚愚	490	3
深圳华大基因研究院	王俊	470	3
中国科学技术大学	郭国平	458	5
福建农林大学	尤民生	436.5	9
清华大学	朱静	424.2	12
北京大学	肖瑞平	398	3
西安交通大学	程海	380	3
中国农业大学	赵要风	310	3
中国科学院上海生物研究所	刘默芳	290	5
中国科学院动物研究所	林鑫华	263	2
大连理工大学	唐莉	247	2
清华大学	吴耀炯	219	3
东南大学	韩俊海	150	3
中国科学院化学研究所	王栋	87	2
北京大学	曹春梅	80	2
复旦大学	陈东戎	30	1

首都医科大学	董涛	20	1
东北师范大学	钟思林	20	1

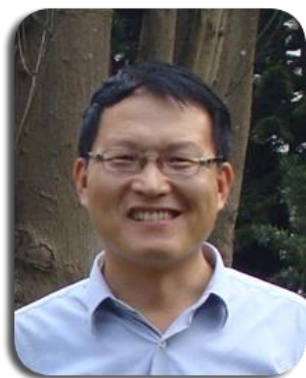
（数据源于 NSFC）

对于 1 月份中国机构发文 CNS 的 27 位通讯作者（统计量不完全），国家自然科学基金项目提供了详细的项目金额和数量。中国科学院化学研究所的万立骏教授以 8970.2 万元高举榜首，项目数为 17 个；中国人民解放军第二军医大学的曹雪涛教授和燕山大学的田永君教授以 2796.4 万和 1577 万分列第二、三名，他们的项目数分别为 17 和 7 个。

排名前 10 的通讯作者分别来自北京（5 位）、上海（2 位）、南京（2 位）和秦皇岛（1 位），其中，北京地区 5 位通讯作者位于项目金额榜前十位之内，这反映出北京位列 1 月份 CNS 中国机构影响因子之首的经费基础。

八、专家精选

The mouse excisional wound splinting model, including applications for stem cell transplantation.（清华大学）



清华大学深圳研究生院吴耀炯教授（左图）经过几年的探索，成功的解决了小鼠伤口模型的皮肤收缩问题，并且针对干细胞移植皮肤再生修复的需求，建立了完善的干细胞移植及观察体系，该成果发表在今年一月份的《nature protocol》中。该实验体系为系统、稳定地观察和分析伤口愈合和干细胞皮肤再生修复奠定了基础。

伤口愈合与皮肤再生研究是现代生物医学研究领域的一个重要分支，其意义不仅在于解释伤口愈合的生物过程，而且具有解决无疤痕伤口愈合和皮肤再生等问题的临床应用意义。伤口愈合是一个极其复杂的过程，受到多种细胞及细胞因子等因素的综合影响。通过几十年的努力，科学家已经对皮肤组织中的多种干细胞及其生物特性的研究取得了巨大进展，为实现伤口的无疤痕愈合和完整功能的人工皮肤的研制创造了条件。

有十多年的干细胞研究经验，早在哈佛大学工作期间，吴教授就开始了干细胞移植组织再生修复研究，并取得了理想的效果，在 *Stem Cells* 等杂志发表大量论文并被广泛引用，部分成果申请美国专利。

Trachea-derived dpp controls adult midgut homeostasis in *Drosophila*. (中国科学院动物研究所)



中国科学院动物研究所林鑫华教授（左图）课题组的研究人员发现了，果蝇气管来源的 BMP 配体 Dpp 在调节中肠稳态中发挥着重要作用，这项研究首次揭示了气管的双面功能，相关成果公布在 *Developmental Cell* 杂志上。

研究表明，Dpp 信号通路主要在果蝇中肠的吸收细胞中激活，而在吸收细胞中抑制 Dpp 信号通路会产生大量的类中肠干细胞及其子代细胞，从而导致肠道稳态丧失。最令人兴奋的是，研究发现 Dpp 信号通路的配体特异地在果蝇的呼吸器官——气管中表达，随着气管细胞穿过基底层肌肉细胞而传递到肠道组织。重要的是，在气管中抑制 Dpp 配体的表达会产生与在吸收细胞中抑制 Dpp 信号通路一致的表型。

这项研究首次揭示了气管不仅负责气体交换的功能，同时还分泌 Dpp 形态发生素来调节肠道组织稳态。这些发现将开辟一个全新的组织间对话影响组织稳态的领域。这必将对今后研究组织间对话、组织稳态、器官重塑、癌症发生等多个领域产生深远的影响。

Neurexin Regulates Visual Function via Mediating Retinoid Transport to Promote Rhodopsin Maturation. (东南大学)

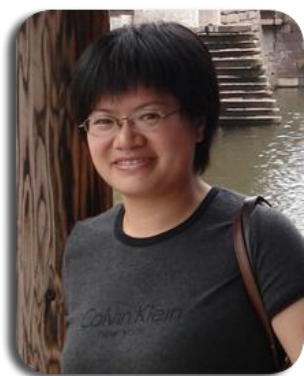


东南大学谢维教授（左图）课题组和韩俊海课题组的研究人员发现了一种重要的突触细胞粘附因子 Neurexins 的新作用——参与视觉功能调控，研究人员发现 Neurexins 能介导视黄醇运输，以及随后的视紫红质成熟过程，并调控脂蛋白水平。相关成果公布在 *Neuron* 杂志上。

在这篇文章中，研究人员发现 α -Neurexin 在果蝇中的同源物，对于果蝇飞行视觉功能十分关键，如果缺失 Neurexin，就会由于视紫红质水平下降，而显著损伤视觉功能。

此外，研究人员还证明了 Neurexin 是确保载脂蛋白水平必不可少的作用因子。结果揭示出了 Neurexin 在介导视黄醇运输，以及随后的视紫红质成熟过程中的作用，并指出了 Neurexin 具有调节脂蛋白的功能。

piRNA-Triggered MIWI Ubiquitination and Removal by APC/C in Late Spermatogenesis. (中国科学院上海生命科学研究院)



中国科学院上海生命科学研究院刘默芳研究员（左图）和王恩多院士在新研究中证实，piRNA 在精子发生后期通过 APC/C 触发了 MIWI 泛素化及 MIWI/piRNA 机器清除。这一研究发现对于深入了解 piRNA 作用通路在哺乳动物精子发生中的功能机制具有重要意义。相关论文发表在 1 月 14 日的《发育生物学》(*Developmental Cell*) 杂志上。

在这篇文章中，研究人员证实小鼠 PIWI (MIWI) 是通过 APC/C-26S 蛋白酶体信号通路进行降解，piRNAs 通过促进 MIWI 与一种 APC/C 底物结合亚基的互作在这一过程中发挥了至关重要的作用。有趣的是，研究人员发现在晚期精细胞中 piRNA 触发的 MIWI 破坏，转而导致了 piRNA 消除，这揭示了一条在特定的发育阶段调节性清除 MIWI/piRNA 机器的前馈机

制。重要的是，研究人员发现适当清除 MIWI/piRNA 是精子成熟的必要条件。

这些结果表明 piRNAs 通过泛素-蛋白酶体信号通路调控了 MIWI/piRNA 机器的清除，证实
在雄性生殖细胞发育过程中适当的时序调控 MIWI/piRNA 具有非常重要的意义。

Interferon-induced transmembrane protein-3 genetic variant rs12252-C is associated with severe influenza in Chinese individuals. (首都医科大学)



由中国首都医科大学董涛教授（左图）领导的国际研究小组，发现了一种常见于中国人群的遗传变异 rs12252-C，这一研究发现这或许有助于阐明某些猪流感感染者会得重病的原因，并以此改变他们的治疗方式。相关研究发表在 1 月 29 日的《自然通讯》（Nature Communications）杂志上

在这篇文章中，来自中国和英国的研究人员对 2009-2010 年猪流感大流行期间住进北京一家医院的 83 名患者进行了分析。在具有肺炎、呼吸或肾脏衰竭等严重并发症的患者中，69% 的人携带这一遗传改变。而病症轻微的患者中，只有 25% 的人有这一遗传突变。

研究作者之一、牛津大学 Weatherall 分子医学研究所主任 Andrew McMichael 说：“这并不意味着如果你有这一基因变异就应该感到恐慌。大多数有此变异的人并不会遭遇到麻烦。这是因为，这一基因改变并不会让人们得流感的可能性增加，毕竟还要考虑环境接触和早先免疫等其他因素。不过具有这一遗传变异的人一旦受到感染，其患重病的可能性要高 5-6”。

九、1 月份论文列表

1、Nature 及其子刊

Divergent global precipitation changes induced by natural versus anthropogenic forcing. [论文链接]

通讯作者：Jian Liu (南京师范大学) Nature. 2013 Jan 31;493(7434):656-9.

As a result of global warming, precipitation is likely to increase in high latitudes and the tropics and to decrease in already dry subtropical regions. The absolute magnitude and regional details of such changes, however, remain intensely debated. As is well known from El Niño studies, sea-surface-temperature gradients across the tropical Pacific Ocean can strongly influence global rainfall. Palaeoproxy evidence indicates that the difference between the warm west Pacific and the colder east Pacific increased in past periods when the Earth warmed as a result of increased solar radiation. In contrast, in most model projections of future greenhouse warming this gradient weakens. It has not been clear how to reconcile these two findings. Here we show in climate model simulations that the tropical Pacific sea-surface-temperature gradient increases when the warming is due to increased solar radiation and decreases when it is due to increased greenhouse-gas forcing. For the same global surface temperature increase the latter pattern produces less rainfall, notably over tropical land, which explains why in the model the late twentieth century is warmer than in the Medieval Warm Period (around AD 1000-1250) but precipitation is less. This difference is consistent with the global tropospheric energy budget, which requires a balance between the latent heat released in precipitation and radiative cooling. The tropospheric cooling is less for increased greenhouse gases, which add radiative absorbers to the troposphere, than for increased solar heating, which is concentrated at the Earth's surface. Thus warming due to increased greenhouse gases produces a climate signature different from that of warming due to solar radiation changes.

The evolution and pathogenic mechanisms of the rice sheath blight pathogen. [[论文链接](#)]

通讯作者：李平&郑爱萍(四川农业大学) Nat Commun. 2013 Jan 29;4:1424.

Rhizoctonia solani is a major fungal pathogen of rice (*Oryza sativa* L.) that causes great yield losses in all rice-growing regions of the world. Here we report the draft genome sequence of the rice sheath blight disease pathogen, *R. solani* AG1 IA, assembled using next-generation Illumina Genome Analyser sequencing technologies. The genome encodes a large and diverse set of secreted proteins, enzymes of primary and secondary metabolism, carbohydrate-active enzymes, and transporters, which probably reflect an exclusive necrotrophic lifestyle. We find few repetitive elements, a closer relationship to Agaricomycotina among Basidiomycetes, and expand protein domains and families. Among the 25 candidate pathogen effectors identified according to their functionality and evolution, we validate 3 that trigger crop defence responses; hence we reveal the exclusive expression patterns of the pathogenic determinants during host infection.

Interferon-induced transmembrane protein-3 genetic variant rs12252-C is associated with severe influenza in Chinese individuals. [[论文链接](#)]

通讯作者：董涛 (首都医科大学) Nat Commun. 2013 Jan 29;4:1418.

The SNP rs12252-C allele alters the function of interferon-induced transmembrane protein-3 increasing the disease severity of influenza virus infection in Caucasians, but the allele is rare. However, rs12252-C is much more common in Han Chinese. Here we report that the CC genotype is found in 69% of Chinese patients with severe pandemic influenza A H1N1/09 virus infection

compared with 25% in those with mild infection. Specifically, the CC genotype was estimated to confer a sixfold greater risk for severe infection than the CT and TT genotypes. More importantly, because the risk genotype occurs with such a high frequency, its effect translates to a large population-attributable risk of 54.3% for severe infection in the Chinese population studied compared with 5.4% in Northern Europeans. Interferon-induced transmembrane protein-3 genetic variants could, therefore, have a strong effect of the epidemiology of influenza in China and in people of Chinese descent.

Climate change patterns in Amazonia and biodiversity. [[论文链接](#)]

通讯作者：程海 (西安交通大学) Nat Commun. 2013 Jan 29;4:1411

Precise characterization of hydroclimate variability in Amazonia on various timescales is critical to understanding the link between climate change and biodiversity. Here we present absolute-dated speleothem oxygen isotope records that characterize hydroclimate variation in western and eastern Amazonia over the past 250 and 20 ka, respectively. Although our records demonstrate the coherent millennial-scale precipitation variability across tropical-subtropical South America, the orbital-scale precipitation variability between western and eastern Amazonia exhibits a quasi-dipole pattern. During the last glacial period, our records imply a modest increase in precipitation amount in western Amazonia but a significant drying in eastern Amazonia, suggesting that higher biodiversity in western Amazonia, contrary to 'Refugia Hypothesis', is maintained under relatively stable climatic conditions. In contrast, the glacial-interglacial climatic perturbations might have been instances of loss rather than gain in biodiversity in eastern Amazonia, where forests may have been more susceptible to fragmentation in response to larger swings in hydroclimate.

Ultrafast universal quantum control of a quantum-dot charge qubit using Landau-Zener-Stückelberg interference. [[论文链接](#)]

通讯作者：郭国平 (中国科学技术大学) Nat Commun. 2013 Jan 29;4:1401

A basic requirement for quantum information processing is the ability to universally control the state of a single qubit on timescales much shorter than the coherence time. Although ultrafast optical control of a single spin has been achieved in quantum dots, scaling up such methods remains a challenge. Here we demonstrate complete control of the quantum-dot charge qubit on the picosecond scale, orders of magnitude faster than the previously measured electrically controlled charge- or spin-based qubits. We observe tunable qubit dynamics in a charge-stability diagram, in a time domain, and in a pulse amplitude space of the driven pulse. The observations are well described by Landau-Zener-Stückelberg interference. These results establish the feasibility of a full set of all-electrical single-qubit operations. Although our experiment is carried out in a solid-state architecture, the technique is independent of the physical encoding of the quantum information and has the potential for wider applications.

Quantitative experimental determination of site-specific magnetic structures by transmitted electrons. [[论文链接](#)]

通讯作者：钟虓葵&朱静 (清华大学) Nat Commun. 2013 Jan 29;4:1395.

Understanding the magnetic structure of materials on a nanometre scale provides fundamental information in the development of novel applications. Here we show a site-specific electron energy-loss magnetic chiral dichroism method, first experimentally demonstrating that the use of transmitted electrons allows us to quantitatively determine atomic site-specific magnetic structure information on a nanometre scale. From one NiFe(2)O(4) nanograin in composite films, we extract its atomic site-specific magnetic circular dichroism spectra and achieve the quantitative magnetic structure information, such as site-specific total magnetic moments and orbital to spin magnetic moment ratios, by constructively selecting the specific dynamical diffraction conditions in electron energy-loss magnetic chiral dichroism experiments. The site-specific electron energy-loss magnetic chiral dichroism method shows its unique ability for solving the site-specific magnetic structure at nanoscale resolution, compared with X-ray magnetic circular dichroism and neutron diffraction. This work opens a door to meet the challenge of exploring the magnetic structures of magnetic materials at the nanoscale using transmitted electrons.

Erbin interacts with TARP γ -2 for surface expression of AMPA receptors in cortical interneurons. [[论文链接](#)]

通讯作者：梅林 (杭州师范大学) Nat Neurosci. 2013 Jan 27.

Inhibitory neurons control the firing of glutamatergic neurons and synchronize brain activity. However, little is known about mechanisms of excitatory synapse formation in inhibitory neurons. Here we demonstrate that Erbin is specifically expressed in cortical inhibitory neurons. It localizes at excitatory synapses and regulates AMPA receptor (AMPA) surface expression. Erbin mutation reduced mEPSCs and AMPAR currents specifically in parvalbumin (PV)-positive interneurons but not in pyramidal neurons. We found that the AMPAR auxiliary protein TARP γ -2 was specifically expressed in cortical interneurons. Erbin interacts with TARP γ -2 and is crucial for its stability. Deletion of the γ -2-interacting domain in Erbin attenuated surface AMPAR and excitatory transmission in PV-positive interneurons. Furthermore, we observed behavioral deficits in Erbin-null mice and in mice expressing an Erbin truncation mutant that is unable to interact with TARP γ -2. These observations demonstrate a crucial function for Erbin in AMPAR surface expression in cortical PV-positive interneurons and may contribute to a better understanding of psychiatric disorders.

Single-base resolution methylomes of tomato fruit development reveal epigenome modifications associated with ripening. [[论文链接](#)]

通讯作者：钟思林 (东北师范大学) Nat Biotechnol. 2013 Jan 27;31(2):154-9

Ripening of tomato fruits is triggered by the plant hormone ethylene, but its effect is restricted by an unknown developmental cue to mature fruits containing viable seeds. To determine whether this cue involves epigenetic remodeling, we expose tomatoes to the methyltransferase inhibitor 5-azacytidine and find that they ripen prematurely. We performed whole-genome bisulfite sequencing on fruit in four stages of development, from immature to ripe. We identified 52,095 differentially methylated regions (representing 1% of the genome) in the 90% of the genome covered by our analysis. Furthermore, binding sites for RIN, one of the main ripening transcription factors, are frequently localized in the demethylated regions of the promoters of numerous ripening genes, and binding occurs in concert with demethylation. Our data show that the epigenome is not static during development and may have been selected to ensure the fidelity of developmental processes such as ripening. Crop-improvement strategies could benefit by taking into account not only DNA sequence variation among plant lines, but also the information encoded in the epigenome.

Central role of E3 ubiquitin ligase MG53 in insulin resistance and metabolic disorders. [[论文链接](#)]

通讯作者：肖瑞平&曹春梅 (北京大学) Nature. 2013 Jan 27.

Insulin resistance is a fundamental pathogenic factor present in various metabolic disorders including obesity and type 2 diabetes. Although skeletal muscle accounts for 70-90% of insulin-stimulated glucose disposal, the mechanism underlying muscle insulin resistance is poorly understood. Here we show in mice that muscle-specific mitsugumin 53 (MG53; also called TRIM72) mediates the degradation of the insulin receptor and insulin receptor substrate 1 (IRS1), and when upregulated, causes metabolic syndrome featuring insulin resistance, obesity, hypertension and dyslipidaemia. MG53 expression is markedly elevated in models of insulin resistance, and MG53 overexpression suffices to trigger muscle insulin resistance and metabolic syndrome sequentially. Conversely, ablation of MG53 prevents diet-induced metabolic syndrome by preserving the insulin receptor, IRS1 and insulin signalling integrity. Mechanistically, MG53 acts as an E3 ligase targeting the insulin receptor and IRS1 for ubiquitin-dependent degradation, comprising a central mechanism controlling insulin signal strength in skeletal muscle. These findings define MG53 as a novel therapeutic target for treating metabolic disorders and associated cardiovascular complications.

Reduced plumage and flight ability of a new Jurassic paravian theropod from China. [[论文链接](#)]

通讯作者：Pascal Godefroit (吉林大学) Nat Commun. 2013 Jan 22;4:1394.

Feathered theropods were diverse in the Early Cretaceous Jehol Group of western Liaoning Province, China. Recently, anatomically distinct feathered taxa have been discovered in the older Middle-Late Jurassic Tiaojishan Formation in the same region. Phylogenetic hypotheses including these specimens have challenged the pivotal position of Archaeopteryx in bird phylogeny. Here we report a basal troodontid from the Tiaojishan Formation that resembles Anchiornis, also from

Jianchang County (regarded as sister-taxa). The feathers of Eosinopteryx are less extensive on the limbs and tail than Anchiornis and other deinonychosaurs. With reduced plumage and short uncurved pedal claws, Eosinopteryx would have been able to run unimpeded (with large foot remiges cursorial locomotion was likely problematic for Anchiornis). Eosinopteryx increases the known diversity of small-bodied dinosaurs in the Jurassic, shows that taxa with similar body plans could occupy different niches in the same ecosystem and suggests a more complex picture for the origin of flight.

Globally homochiral assembly of two-dimensional molecular networks triggered by co-absorbers.[\[论文链接\]](#)

通讯作者：万立骏&王栋(中国科学院化学研究所) Nat Commun. 2013 Jan 22;4:1389

Understanding the chirality induction and amplification processes, and the construction of globally homochiral surfaces, represent essential challenges in surface chirality studies. Here we report the induction of global homochirality in two-dimensional enantiomorphous networks of achiral molecules via co-assembly with chiral co-absorbers. The scanning tunnelling microscopy investigations and molecular mechanics simulations demonstrate that the point chirality of the co-absorbers transfers to organizational chirality of the assembly units via enantioselective supramolecular interactions, and is then hierarchically amplified to the global homochirality of two-dimensional networks. The global homochirality of the network assembly shows nonlinear dependence on the enantiomeric excess of chiral co-absorber in the solution phase, demonstrating, for the first time, the validation of the 'majority rules' for the homochirality control of achiral molecules at the liquid/solid interface. Such an induction and nonlinear chirality amplification effect promises a new approach towards two-dimensional homochirality control and may reveal important insights into asymmetric heterogeneous catalysis, chiral separation and chiral crystallization.

Quantum-coupled radial-breathing oscillations in double-walled carbon nanotubes. [\[论文链接\]](#)

通讯作者：王峰 (中国科学院物理研究所) Nat Commun. 2013 Jan 22;4:1375

Van der Waals-coupled materials, ranging from multilayers of graphene and MoS(2) to superlattices of nanoparticles, exhibit rich emerging behaviour owing to quantum coupling between individual nanoscale constituents. Double-walled carbon nanotubes provide a model system for studying such quantum coupling mediated by van der Waals interactions, because each constituent single-walled nanotube can have distinctly different physical structures and electronic properties. Here we systematically investigate quantum-coupled radial-breathing mode oscillations in chirality-defined double-walled nanotubes by combining simultaneous structural, electronic and vibrational characterizations on the same individual nanotubes. We show that these radial-breathing oscillations are collective modes characterized by concerted inner- and outer-wall motions, and determine quantitatively the tube-dependent van der Waals potential governing their vibration frequencies. We also observe strong quantum interference between Raman scattering

from the inner- and outer-wall excitation pathways, the relative phase of which reveals chirality-dependent excited-state potential energy surface displacement in different nanotubes.

Visualizing the atomic-scale electronic structure of the $\text{Ca}_2\text{CuO}_2\text{Cl}_2$ Mott insulator. [[论文链接](#)]

通讯作者：王亚愚 (清华大学) Nat Commun. 2013 Jan 22;4:1365

Although the mechanism of superconductivity in the cuprates remains elusive, it is generally agreed that at the heart of the problem is the physics of doped Mott insulators. A crucial step for solving the high temperature superconductivity puzzle is to elucidate the electronic structure of the parent compound and the behaviour of doped charge carriers. Here we use scanning tunnelling microscopy to investigate the atomic-scale electronic structure of the $\text{Ca}_2\text{CuO}_2\text{Cl}_2$ parent Mott insulator of the cuprates. The full electronic spectrum across the Mott-Hubbard gap is uncovered for the first time, which reveals the particle-hole symmetric and spatially uniform Hubbard bands. Defect-induced charge carriers are found to create broad in-gap electronic states that are strongly localized in space. We show that the electronic structure of pristine Mott insulator is consistent with the Zhang-Rice singlet model, but the peculiar features of the doped electronic states require further investigations.

The mouse excisional wound splinting model, including applications for stem cell transplantation. [[论文链接](#)]

通讯作者：吴耀炯 (清华大学) Nat Protoc. 2013 Jan 17;8(2):302-9.

The mouse excisional wound healing model has been used extensively to study wound healing and cutaneous regeneration. However, as mouse skin is mobile, contraction accounts for a large part of wound closure. In the mouse excisional wound splinting model, a splinting ring tightly adheres to the skin around the wound, preventing local skin contraction. The wound therefore heals through granulation and re-epithelialization, a process similar to that occurring in humans. The model, which takes 2-4 weeks to carry out, can be used to study the effects of stem cells on cutaneous repair or regeneration. In this protocol, we also describe how to implant stem cells onto the wound bed in Matrigel and/or into the surrounding tissue through injection. Serial wound tissue samples at different time points can be harvested to monitor the engraftment and the effects of stem cells in angiogenesis and wound healing.

Ultrahard nanotwinned cubic boron nitride. [[论文链接](#)]

通讯作者：田永君 (燕山大学) Nature. 2013 Jan 17;493(7432):385-8

Cubic boron nitride (cBN) is a well known superhard material that has a wide range of industrial applications. Nanostructuring of cBN is an effective way to improve its hardness by virtue of the Hall-Petch effect--the tendency for hardness to increase with decreasing grain size. Polycrystalline cBN materials are often synthesized by using the martensitic transformation of a graphite-like BN

precursor, in which high pressures and temperatures lead to puckering of the BN layers. Such approaches have led to synthetic polycrystalline cBN having grain sizes as small as ~ 14 nm (refs 1, 2, 4, 5). Here we report the formation of cBN with a nanostructure dominated by fine twin domains of average thickness ~ 3.8 nm. This nanotwinned cBN was synthesized from specially prepared BN precursor nanoparticles possessing onion-like nested structures with intrinsically puckered BN layers and numerous stacking faults. The resulting nanotwinned cBN bulk samples are optically transparent with a striking combination of physical properties: an extremely high Vickers hardness (exceeding 100 GPa, the optimal hardness of synthetic diamond), a high oxidation temperature ($\sim 1,294$ °C) and a large fracture toughness (>12 MPa m^{1/2}), well beyond the toughness of commercial cemented tungsten carbide, ~ 10 MPa m^{1/2}). We show that hardening of cBN is continuous with decreasing twin thickness down to the smallest sizes investigated, contrasting with the expected reverse Hall-Petch effect below a critical grain size or the twin thickness of ~ 10 -15 nm found in metals and alloys.

Visualization and quantification of transition metal atomic mixing in Mo(1-x)W(x)S(2) single layers. [[论文链接](#)]

通讯作者: Kazu Suenaga (国立台湾科技大学) Nat Commun. 2013 Jan 15;4:1351

The alloying behaviour of materials is a well-known problem in all kinds of compounds. Revealing the heteroatomic distributions in two-dimensional crystals is particularly critical for their practical use as nano-devices. Here we obtain statistics of the homo- and heteroatomic coordinates in single-layered Mo(1-x)W(x)S(2) from the atomically resolved scanning transmission electron microscope images and successfully quantify the degree of alloying for the transition metal elements (Mo or W). The results reveal the random alloying of this mixed dichalcogenide system throughout the chemical compositions ($x=0$ to 1). Such a direct route to gain an insight into the alloying degree on individual atom basis will find broad applications in characterizing low-dimensional heterocompounds and become an important complement to the existing theoretical methods.

A heterozygous moth genome provides insights into herbivory and detoxification. [[论文链接](#)]

通讯作者: 尤民生&王俊(福建农林大学&深圳华大基因研究院) Nat Genet. Epub 2013 Jan 13.

How an insect evolves to become a successful herbivore is of profound biological and practical importance. Herbivores are often adapted to feed on a specific group of evolutionarily and biochemically related host plants, but the genetic and molecular bases for adaptation to plant defense compounds remain poorly understood. We report the first whole-genome sequence of a basal lepidopteran species, *Plutella xylostella*, which contains 18,071 protein-coding and 1,412 unique genes with an expansion of gene families associated with perception and the detoxification of plant defense compounds. A recent expansion of retrotransposons near detoxification-related genes and a wider system used in the metabolism of plant defense compounds are shown to also be involved in the development of insecticide resistance. This work shows the genetic and molecular bases for the evolutionary success of this worldwide herbivore and offers wider insights

into insect adaptation to plant feeding, as well as opening avenues for more sustainable pest management.

Extensive diversification of IgH subclass-encoding genes and IgM subclass switching in crocodilians. [[论文链接](#)]

通讯作者：赵要风(中国农业大学)Nat Commun. 2013 Jan 8;4:1337.

Crocodilians are a group of reptiles that are closely related to birds and are thought to possess a strong immune system. Here we report that the IgH locus in the Siamese crocodile and the Chinese alligator contains multiple μ genes, in contrast to other tetrapods. Both the $\mu 2$ and $\mu 3$ genes are expressed through class-switch recombination involving the switch region and germline transcription. Both IgM1 and IgM2 are present in the serum as polymers, which implies that IgM class switching may have significant roles in humoral immunity. The crocodilian α genes are the first IgA-encoding genes identified in reptiles, and these genes show an inverted transcriptional orientation similar to that of birds. The identification of both α and δ genes in crocodilians suggests that the IgH loci of modern living mammals, reptiles and birds share a common ancestral organization.

A thermoresponsive and chemically defined hydrogel for long-term culture of human embryonic stem cells [[论文链接](#)]

通讯作者：Rong Zhang (常州大学)Nat Commun. 2013 Jan 8;4:1335

Cultures of human embryonic stem cell typically rely on protein matrices or feeder cells to support attachment and growth, while mechanical, enzymatic or chemical cell dissociation methods are used for cellular passaging. However, these methods are ill defined, thus introducing variability into the system, and may damage cells. They also exert selective pressures favouring cell aneuploidy and loss of differentiation potential. Here we report the identification of a family of chemically defined thermoresponsive synthetic hydrogels based on 2-(diethylamino)ethyl acrylate, which support long-term human embryonic stem cell growth and pluripotency over a period of 2-6 months. The hydrogels permitted gentle, reagent-free cell passaging by virtue of transient modulation of the ambient temperature from 37 to 15 °C for 30 min. These chemically defined alternatives to currently used, undefined biological substrates represent a flexible and scalable approach for improving the definition, efficacy and safety of human embryonic stem cell culture systems for research, industrial and clinical applications.

Recoding RNA editing of AZIN1 predisposes to hepatocellular carcinoma. [[论文链接](#)]

通讯作者：关新元 (香港大学)Nat Med. Epub 2013 Jan 6.

A better understanding of human hepatocellular carcinoma (HCC) pathogenesis at the molecular level will facilitate the discovery of tumor-initiating events. Transcriptome sequencing revealed that adenosine-to-inosine (A→I) RNA editing of AZIN1 (encoding antizyme inhibitor 1) is

increased in HCC specimens. A→I editing of AZIN1 transcripts, specifically regulated by ADAR1 (encoding adenosine deaminase acting on RNA-1), results in a serine-to-glycine substitution at residue 367 of AZIN1, located in β -strand 15 (β 15) and predicted to cause a conformational change, induced a cytoplasmic-to-nuclear translocation and conferred gain-of-function phenotypes that were manifested by augmented tumor-initiating potential and more aggressive behavior. Compared with wild-type AZIN1 protein, the edited form has a stronger affinity to antizyme, and the resultant higher AZIN1 protein stability promotes cell proliferation through the neutralization of antizyme-mediated degradation of ornithine decarboxylase (ODC) and cyclin D1 (CCND1). Collectively, A→I RNA editing of AZIN1 may be a potential driver in the pathogenesis of human cancers, particularly HCC.

2、Cell 及其子刊

Induction of Siglec-G by RNA Viruses Inhibits the Innate Immune Response by Promoting RIG-I Degradation. [\[论文链接\]](#)

通讯作者：曹雪涛 (浙江大学)Cell. 2013 Jan 31;152(3):467-78.

RIG-I is a critical RNA virus sensor that serves to initiate antiviral innate immunity. However, posttranslational regulation of RIG-I signaling remains to be fully understood. We report here that RNA viruses, but not DNA viruses or bacteria, specifically upregulate lectin family member Siglec-G expression in macrophages by RIG-I- or NF- κ B-dependent mechanisms. Siglec-G-induced recruitment of SHP2 and the E3 ubiquitin ligase c-Cbl to RIG-I leads to RIG-I degradation via K48-linked ubiquitination at Lys813 by c-Cbl. By increasing type I interferon production, targeted inactivation of Siglec-G protects mice against lethal RNA virus infection. Taken together, our data reveal a negative feedback loop of RIG-I signaling and identify a Siglec-G-mediated immune evasion pathway exploited by RNA viruses with implication in antiviral applications. These findings also provide insights into the functions and crosstalk of Siglec-G, a known adaptive response regulator, in innate immunity.

Trachea-derived dpp controls adult midgut homeostasis in Drosophila. [\[论文链接\]](#)

通讯作者：林鑫华 (中国科学院动物研究所)Dev Cell. 2013 Jan 28;24(2):133-43

Homeostasis in adult tissues is maintained by resident stem cells and their progeny. Little is known about the regulation of tissue homeostasis by organ-organ interaction. Here we demonstrate that trachea-derived Decapentaplegic (Dpp), the main bone morphogenetic protein ligand in Drosophila, is essential for adult midgut homeostasis. We show that Dpp signaling is primarily activated in enterocytes (ECs). Depletion of Dpp signaling in ECs results in excess amounts of intestinal stem-cell-like cells and their progeny. Importantly, we find that Dpp is expressed specifically in tracheal cells that reach the intestinal cells through the visceral muscles. Depletion of dpp expression in tracheal cells phenocopies the Dpp loss-of-function defects in ECs.

Our data demonstrate that the *Drosophila* trachea not only exchanges air for bodily needs but also produces a Dpp morphogen essential for neighboring tissue homeostasis. This work will provide important insights into the mechanisms of tissue homeostasis control by interorgan communication.

Neurexin Regulates Visual Function via Mediating Retinoid Transport to Promote Rhodopsin Maturation. [\[论文链接\]](#)

通讯作者：谢维&韩俊海 (东南大学)Neuron. 2013 Jan 23;77(2):311-22

Neurexins are cell adhesion molecules involved in synapse formation and synaptic regulation. Mutations in the neurexin genes are linked to a number of neurodevelopmental disorders such as autism. Here, we show that the *Drosophila* homolog of α -Neurexin is critical for fly visual function. Lack of Neurexin leads to significantly impaired visual function due to reduced rhodopsin levels. We show that the decreased chromophore levels cause deficits in rhodopsin maturation and that Neurexin is required for retinoid transport. Using yeast two-hybrid screening, we identify that Neurexin interacts with apolipoprotein I (ApoL I), a product generated by cleavage of retinoid- and fatty acid-binding glycoprotein (RFABG) that functions in retinoid transport. Finally, we demonstrate that Neurexin is essential for the apolipoproteins level. Our results reveal a role for Neurexin in mediating retinoid transport and subsequent rhodopsin maturation and suggest that Neurexin regulates lipoprotein function.

Elucidation of the Biosynthetic Gene Cluster and the Post-PKS Modification Mechanism for Fostriecin in *Streptomyces pulveraceus*. [\[论文链接\]](#)

通讯作者：邱荣国&唐莉 (大连理工大学)Chem Biol. 2013 Jan 24;20(1):45-54

Fostriecin is a unique phosphate monoester antibiotic that was isolated from *Streptomyces pulveraceus* as a protein phosphatase 2A (PP2A) and PP4A selective inhibitor. However, its biosynthetic mechanism remains to be elucidated. In this study, a 73 kb gene cluster encoding a six modular Type I polyketide synthases (PKS) and seven tailoring enzymes was identified by cosmid sequencing from the producer. The functions of two tailoring enzymes were characterized by gene disruption and an in vitro enzyme activity assay. Remarkably, the isolation of three malonylated fostriecin analogs from post-PKS gene knockout mutants indicated malonylated-polyketide formation could be a normal biosynthetic process in the formation of the unsaturated six-membered lactone in fostriecin. Based on this study, a comprehensive post-PKS modification mechanism for fostriecin biosynthesis was proposed.

Olig2 targets chromatin remodelers to enhancers to initiate oligodendrocyte differentiation. [\[论文链接\]](#)

通讯作者：Q. Richard Lu (四川大学)Cell. 2013 Jan 17;152(1-2):248-61

Establishment of oligodendrocyte identity is crucial for subsequent events of myelination in the

CNS. Here, we demonstrate that activation of ATP-dependent SWI/SNF chromatin-remodeling enzyme Smarca4/Brg1 at the differentiation onset is necessary and sufficient to initiate and promote oligodendrocyte lineage progression and maturation. Genome-wide multistage studies by ChIP-seq reveal that oligodendrocyte-lineage determination factor Olig2 functions as a pre patterning factor to direct Smarca4/Brg1 to oligodendrocyte-specific enhancers. Recruitment of Smarca4/Brg1 to distinct subsets of myelination regulatory genes is developmentally regulated. Functional analyses of Smarca4/Brg1 and Olig2 co-occupancy relative to chromatin epigenetic marking uncover stage-specific cis-regulatory elements that predict sets of transcriptional regulators controlling oligodendrocyte differentiation. Together, our results demonstrate that regulation of the functional specificity and activity of a Smarca4/Brg1-dependent chromatin-remodeling complex by Olig2, coupled with transcriptionally linked chromatin modifications, is critical to precisely initiate and establish the transcriptional program that promotes oligodendrocyte differentiation and subsequent myelination of the CNS.

Riboswitch control of aminoglycoside antibiotic resistance.[\[论文链接\]](#)

通讯作者：陈东戎 (复旦大学)Cell. 2013 Jan 17;152(1-2):68-81.

The majority of riboswitches are regulatory RNAs that regulate gene expression by binding small-molecule metabolites. Here we report the discovery of an aminoglycoside-binding riboswitch that is widely distributed among antibiotic-resistant bacterial pathogens. This riboswitch is present in the leader RNA of the resistance genes that encode the aminoglycoside acetyl transferase (AAC) and aminoglycoside adenylyl transferase (AAD) enzymes that confer resistance to aminoglycoside antibiotics through modification of the drugs. We show that expression of the AAC and AAD resistance genes is regulated by aminoglycoside binding to a secondary structure in their 5' leader RNA. Reporter gene expression, direct measurements of drug RNA binding, chemical probing, and UV crosslinking combined with mutational analysis demonstrate that the leader RNA functions as an aminoglycoside-sensing riboswitch in which drug binding to the leader RNA leads to the induction of aminoglycosides antibiotic resistance.

piRNA-Triggered MIWI Ubiquitination and Removal by APC/C in Late Spermatogenesis.
[\[论文链接\]](#)

通讯作者：刘默芳&王恩多 (中国科学院上海生物研究所)Dev Cell. 2013 Jan 14;24(1):13-25.

The PIWI/PIWI-interacting RNA (piRNA) machinery has been well documented to maintain genome integrity by silencing transposons in animal germ cells. Recent studies have advanced our understanding of the biogenesis and function of this machinery; however, its metabolism has remained largely unexplored. Here, we show that murine PIWI (MIWI) is degraded through the APC/C-26S proteasome pathway and that piRNAs play an indispensable role in this process by enhancing MIWI interaction with an APC/C substrate-binding subunit. Interestingly, piRNA-triggered MIWI destruction occurs in late spermatids, which in turn leads to piRNA elimination, suggesting a feedforward mechanism for coordinated removal of the MIWI/piRNA

machinery at a specific developmental stage. Importantly, the proper removal of MIWI/piRNA is essential for sperm maturation. Together, our results reveal a role for piRNAs in regulating the clearance of the MIWI/piRNA machinery via the ubiquitin-proteasome pathway and demonstrate the critical importance of proper temporal regulation of MIWI/piRNA in male germ cell development.

Direct Conversion of Fibroblasts to Neurons by Reprogramming PTB-Regulated MicroRNA Circuits.[\[论文链接\]](#)

通讯作者：傅向东 (武汉大学)Cell. 2013 Jan 17;152(1-2):82-96.

The induction of pluripotency or trans-differentiation of one cell type to another can be accomplished with cell-lineage-specific transcription factors. Here, we report that repression of a single RNA binding polypyrimidine-tract-binding (PTB) protein, which occurs during normal brain development via the action of miR-124, is sufficient to induce trans-differentiation of fibroblasts into functional neurons. Besides its traditional role in regulated splicing, we show that PTB has a previously undocumented function in the regulation of microRNA functions, suppressing or enhancing microRNA targeting by competitive binding on target mRNA or altering local RNA secondary structure. A key event during neuronal induction is the relief of PTB-mediated blockage of microRNA action on multiple components of the REST complex, thereby derepressing a large array of neuronal genes, including miR-124 and multiple neuronal-specific transcription factors, in nonneuronal cells. This converts a negative feedback loop to a positive one to elicit cellular reprogramming to the neuronal lineage.

Decorating proteins with "sweets" is a flexible matter.[\[论文链接\]](#)

通讯作者：Mingjie Zhang (香港科技大学)Structure. 2013 Jan 8;21(1):1-2.

In this issue of Structure, Nyirenda and colleagues use a combination of X-ray and NMR to demonstrate that ms timescale conformational dynamics of oligosaccharyltransferases are critical for N-linked protein glycosylation.

c-Cbl-Mediated Neddylolation Antagonizes Ubiquitination and Degradation of the TGF- β Type II Receptor.[\[论文链接\]](#)

通讯作者：陈晔光 (清华大学)Mol Cell. Epub 2013 Jan 1.

Transforming growth factor β (TGF- β) is a potent antiproliferative factor in multiple types of cells. Deregulation of TGF- β signaling is associated with the development of many cancers, including leukemia, though the molecular mechanisms are largely unclear. Here, we show that Casitas B-lineage lymphoma (c-Cbl), a known proto-oncogene encoding an ubiquitin E3 ligase, promotes TGF- β signaling by neddylating and stabilizing the type II receptor (T β RII). Knockout of c-Cbl decreases the T β RII protein level and desensitizes hematopoietic stem or progenitor cells to TGF- β stimulation, while c-Cbl overexpression stabilizes T β RII and sensitizes leukemia cells to

TGF- β . c-Cbl conjugates neural precursor cell-expressed, developmentally downregulated 8 (NEDD8), a ubiquitin-like protein, to T β RII at Lys556 and Lys567. Neddylation of T β RII promotes its endocytosis to EEA1-positive early endosomes while preventing its endocytosis to caveolin-positive compartments, therefore inhibiting T β RII ubiquitination and degradation. We have also identified a neddylation-activity-defective c-Cbl mutation from leukemia patients, implying a link between aberrant T β RII neddylation and leukemia development.

3、Science 及其子刊

Diisopropylammonium bromide is a high-temperature molecular ferroelectric crystal[\[论文链接\]](#)

通讯作者：熊仁根 (东南大学) Science. 2013 Jan 25;339(6118):425-8

Molecular ferroelectrics are highly desirable for their easy and environmentally friendly processing, light weight, and mechanical flexibility. We found that diisopropylammonium bromide (DIPAB), a molecular crystal processed from aqueous solution, is a ferroelectric with a spontaneous polarization of 23 microcoulombs per square centimeter [close to that of barium titanate (BTO)], high Curie temperature of 426 kelvin (above that of BTO), large dielectric constant, and low dielectric loss. DIPAB exhibits good piezoelectric response and well-defined ferroelectric domains. These attributes make it a molecular alternative to perovskite ferroelectrics and ferroelectric polymers in sensing, actuation, data storage, electro-optics, and molecular or flexible electronics

Crystalline inorganic frameworks with 56-ring, 64-ring, and 72-ring channels. [\[论文链接\]](#)

通讯作者：王素兰 (国立清华大学) Science. Epub 2013 Jan 24.

The development of zeolite-like structures with extra-large pores (>12-membered rings, 12R) has been sporadic and is currently at 30R. In general, templating via molecules leads to crystalline frameworks, whereas the use of organized assemblies that permit much larger pores produces noncrystalline frameworks. Synthetic methods that generate crystallinity from both discrete templates and organized assemblies represent a viable design strategy for developing crystalline porous inorganic frameworks spanning the micro and meso regimes. We show that by integrating templating mechanisms for both zeolites and mesoporous silica in a single system, the channel size for gallium zincophosphites can be systematically tuned from 24R and 28R to 40R, 48R, 56R, 64R, and 72R. Although the materials have low thermal stability and retain their templating agents, single-activator doping of Mn(2+) can create white-light photoluminescence.

Human CD8+ Regulatory T Cells Inhibit GVHD and Preserve General Immunity in Humanized Mice. [\[论文链接\]](#)

通讯作者: Wenwei Tu (香港大学) Sci Transl Med. 2013 Jan 16;5(168):168ra9.

Graft-versus-host disease (GVHD) is a lethal complication of allogeneic bone marrow transplantation (BMT). Immunosuppressive agents are currently used to control GVHD but may cause general immune suppression and limit the effectiveness of BMT. Adoptive transfer of regulatory T cells (T(regs)) can prevent GVHD in rodents, suggesting a therapeutic potential of T(regs) for GVHD in humans. However, the clinical application of T(reg)-based therapy is hampered by the low frequency of human T(regs) and the lack of a reliable model to test their therapeutic effects *in vivo*. Recently, we successfully generated human alloantigen-specific CD8(hi) T(regs) in a large scale from antigenically naïve precursors *ex vivo* using allogeneic CD40-activated B cells as stimulators. We report a human allogeneic GVHD model established in humanized mice to mimic GVHD after BMT in humans. We demonstrate that *ex vivo*-induced CD8(hi) T(regs) controlled GVHD in an allospecific manner by reducing alloreactive T cell proliferation as well as decreasing inflammatory cytokine and chemokine secretion within target organs through a CTLA-4-dependent mechanism in humanized mice. These CD8(hi) T(regs) induced long-term tolerance effectively without compromising general immunity and graft-versus-tumor activity. Our results support testing of human CD8(hi) T(regs) in GVHD in clinical trials.